Received: 4 June 2021 | Revised: 22 December 2021 | Accepted: 24 January 2022

DOI: 10.1111/ina.12999

ORIGINAL ARTICLE

WILEY

The influence of photochemistry on outdoor to indoor NO_2 in some European museums

Terje Grøntoft

Norwegian Institute for Air Research, Kjeller, Norway

Correspondence
Terje Grøntoft, Norwegian Institute for Air Research, P.O.Box 100, Kjeller NO-2027, Norway.
Email: teg@nilu.no

Funding information
European Commission; the Norwegian Archive, Library and Museum Authority; NILU

Abstract

This paper reports 1 year of monthly average NO_2 indoor to outdoor (I/O) concentrations measured in 10 European museums, and a simple steady-state box model that explains the annual variation. The measurements were performed in the EU FP5 project Master (EVK-CT-2002-00093). The work provides extensive documentation of the annual variation of NO_2 I/O concentration ratios, with ratios above unity in the summer, in situations with no indoor emissions of NO_2. The modelling included the most relevant production and removal processes of NO_2 and showed that the outdoor photolysis was the probable main explanation of the annual trends in the NO_2 I/O concentration ratios.

KEYWORDS
indoor exposure, modelling, museums, nitrogen dioxide, outdoor to indoor concentrations, photochemical reaction

1 | INTRODUCTION

Nitrogen dioxide (NO_2) can harm people's health and cultural heritage materials by its oxidizing and/or acidic effects. People spend much of their time indoors. The sometimes higher indoor as compared to outdoor exposure to NO_2 adds to the total person, and object, exposure. A major motivation for understanding the outdoor to indoor NO_2 concentrations in museums is the degradation due to the atmospheric exposure that has been reported of sensitive art materials. This work provides results from annual monthly measurements of NO_2 I/O ratios in 10 European museums. Then, tentatively, a simple model that can approximate the indoor to outdoor (I/O) ratios of NO_2, and higher than unity ratios that are often observed in the summer, from the outdoor NO_x and O_3 values that are more often available from regulatory measurement stations than indoor measured values. A recent paper reviewed the status of knowledge of indoor NO and NO_2 concentrations and chemistry, among other acids and bases that influence indoor air quality.[1] They stated that "in the absence of indoor sources, I/O concentration ratios of nitrogen monoxide (NO) tend to be close to unity, while those for NO_2 tend to be in the range of 0.7 to 0.9 depending on the air exchange rate and relative humidity." The source of the indoor NO_2 is when excluding indoor emissions that are uncommon in museums, the outdoor NO_x ($NO + NO_2$) emissions and ventilation to the indoors, and the indoor reaction of NO with O_3 to NO_2. Annual NO_2 I/O ratios of unity have been measured in for example the Victoria and Albert Museum in London.[2] Higher indoor than outdoor concentrations of NO_2 have, despite the indoor deposition, been measured in museums[3] in the summer. This was explained by splitting of NO_2 outdoors by ultraviolet (UV) light, to NO and O_3, and reaction back to NO_2 in the relative indoor darkness.

Weschler et al.[4] showed that, in the absence of photolysis, due to the rapid reaction of NO with O_3, only the surplus gas of the two will be present at any one time. The dynamic NO_x-O_3 chemistry happens at similar rates as the typical exchanges of indoor air (~1 h^{-1}), which is a reason why it affects the indoor air quality. With a surplus of O_3 indoors most of the incoming NO will react to NO_2.[1,3,5,6] Indoor NO_2 is a source of nitric (HONO) and nitrous acid (HNO_3) through

heterogeneous and homogeneous reactions. The homogeneous reactions can involve ozone (O_3) and volatile organic compounds. The HONO is mainly released back to the air after formation with water on the surfaces. The HNO_3 can be formed together with HONO on the surfaces or deposit and react on the surfaces after oxidation of NO_2 by O_3 in air.[1,4,7,8,9,10,11] Whereas exposure to peak concentrations can be the most damaging to health, it is the long duration accumulated exposure that is usually considered to damage sensitive heritage materials. Outdoor values of NO_2 are more commonly available than values from indoor measurements. Museums can thus benefit from a simple model to estimate long duration indoor exposure doses from the outdoor concentration values. IAQ (Indoor Air Quality) models that calculate I/O gas concentration ratios, including O_3 and NO_2, have been proposed and tested in many studies. Dynamic models (e.g.,[12-14]) some including advanced chemistry schemes,[5,15,16,17,18] and steady-state models (e.g.,[11,19,20]) have been used. Wang[17] provided a literature review of indoor air modelling involving photolysis. Weschler et al.[4] described and explained the dynamic trends of, the O_3, NO, and NO_2^* (NO_x minus NO) species. Drakou et al.[16] observed higher than unity I/O NO_2^* (NO_2 + HONO + HNO_3 + PAN (peroxyacetyl nitrate) = NO_x minus NO) ratios in a building in Thessaloniki, Greece. They found that this could not fully be explained by the reaction of NO with O_3, but that in "the particular building, which was like a smog chamber, it seemed as if NO was transformed to NO_2 mainly by heterogeneous processes and less through the reaction of O_3 with NO." They hypothesized that NO might be oxidized to NO_2 through heterogeneous reactions involving the formation of HONO, and subsequently homogeneous reactions with OH radicals and VOCs that would "alter all the indoor gas-phase chemistry." They concluded that in this building "there seemed to be at times a contribution to indoor NO_2 from HNO_2 and at times from HNO_3 and PAN, and that the homogeneous chemistry and the heterogeneous removal of air pollutants in the applied model (from Nazaroff and Cass[6]) could not fully explain the interplay among O_3, NO, and NO_2 in the building." Zhou et al.[21] reported concentrations of HONO that were on the level of NO_2 in indoor air. As HONO is expected to have been reported with the NO_2 from the passive sampling performed in this work,[1,22] the here reported "NO_2" should, probably, be interpreted as NO_2 + HONO (it is still described in the following simply as NO_2—as reported from the analysis). The HONO would be a product of the indoor NO_2 which was partly formed by reaction of NO with O_3 (Equation (1) below). The inclusion of HONO with the NO_2 seems thus not to disqualify the performed modelling approximation of the monthly averaged indoor NO_2 (interpreted as NO_2 + HONO). It seems, however, that it may have led to some underestimation of the deposition of the NO_2 (exclusive of the HONO, which would be a product from this additional deposition). The above references testify to the complexity of the indoor NO_x heterogeneous and homogeneous chemistry, which this work did, however, not try to simulate in detail.

The aim of this work was to add comparative annual monthly site data to the evidence of increased, and often higher than unity, summer NO_2 I/O ratios. Then, to investigate if a simplified steady-state NO_2 I/O model, adding the effect of outdoor NO_2 photolysis to the heterogeneous indoor removal, could reasonably explain the monthly averaged NO_2 I/O ratios. The reported NO_2 and O_3 measurements were performed in 10 European museums some years ago, from 2004 to 2005, in the EU Master project.[23] Although NO_2 concentrations have since then decreased somewhat in Europe,[24] the presence of nitrogen oxides (NO_x) is still a major worldwide and European air quality challenge.[25-28] Few data on the annual variation and higher average NO_2 indoor than outdoor concentrations in the summer seems to have been reported. It therefore seemed appropriate to report these results that documents many such cases. The presented steady-state box model simplify the dynamic complexity of the homogeneous NO_x-O_3 chemistry with the purpose of approximating the measured time-integrated gas concentrations, and doses, in a single room.

Practical implications

Outdoor photolysis of NO_2 and indoor back-reaction of NO with O_3 can contribute to higher indoor than outdoor exposures to NO_2 in the summer. This is a health concern, and an objects conservation concern in museums. As indoor NO_2 concentrations are seldom measured, but values for outdoor concentrations are often available from regulatory measurement stations, it is of interest to approximate the expected indoor integrated exposures from the outdoor values, with a relatively simple method that shows reasonable fit to measurements. A model expression for the NO_2 indoor to outdoor ratio including the photolysis effect and meeting these criteria was presented.

Degradation due to the atmospheric exposure to NO_2 and/or O_3 has been reported of sensitive art materials such as pigments, dyes, and inks,[29-36]) textiles (Whitmore and Cass, 1989,[37] paper,[38-40] varnish,[41] and metals[42-44]). The damage might be due to both oxidation by the nitrate radical (NO_3·) and acidic effects of nitric acid (HNO_3). The NO_3 radical will react with both saturated and unsaturated organic compounds and form gaseous and surface adsorbed/dissolved HNO_3. The high water solubility and acidity of HNO_3 means that its potential for reducing the surface pH is high, even at its common low indoor concentrations below one ppb.[1] However, as the O_3 + NO reaction decreases O_3 concentrations as much as it increases the NO_2 concentrations, it seems that the effect of this reaction depends on the relative sensitivity of materials to O_3 versus NO_2 and its reaction products. It has been recommended that the concentrations of the pollution gases in museums should be below measurable levels (1 μg m^{-3} ~ 0.5 ppb), based on the precautionary thinking that there is no lower threshold of their effects and that a "no observed adverse effect level" (NOAEL) has not generally been observed.[45] Different materials are, however, clearly at different risk from exposure to the gases.[45-47] To perform realistic evaluations of the damage risk of materials or objects more specific information is needed about the oxidizing and acidic reactions of the deposited gases. As an example, the longer duration degradation of oil paintings, happens by similar

mechanisms as those involved in the initial curing. The oil-containing paint film changes both by oxidation of unsaturated bonds and by hydrolysis of ester bonds in the oils, with both mechanisms leading to the formation of carboxylic groups and the possibility for subsequent metal complexation and substitution with fatty acids to create the often-whitish disfiguring crystallizations of metal soaps.[48] The oxidation of double bonds can be induced by UV irradiation, and/or, probably, by reaction with oxygen radicals and is accelerated by air pollutants such as NO_2 and SO_2,[49,50] and probably also by O_3 and other oxidants, and progress by autoxidation.[51] The hydrolysis reaction is RH-dependent (Modugno et al., 2019). The influence of the deposition of oxidizing and acidic air pollutants on the detailed mechanisms and practical rates of such reactions in the objects at risk seems, however, in most cases not well known.

2 | EXPERIMENTAL AND SITES

In the EU Master project an extensive field test was carried out to measure, and evaluate, the effect of the air environment and particularly of contaminant gases present indoors, on vulnerable art objects in museums. The measurements were performed indoors and just outdoors of galleries over one year with monthly changing of duplicate passive badge samplers of NO_2 and O_3 of the IVL type (Ferm and Bloom, 2010)[52] in one urban and one rurally located museum in five different European regions represented by six different countries, 10 museums in all (Table 1). The supporting Table S1 provides the museums' materials and site description. In the following, the museums will, for simplicity and as the geographical location is of importance for the NO + O_3 reaction, often be described by their geographical location, given in Table 1, rather than by the full museum name.

The monthly pollution gas uptake was found to be well within the chemical absorption capacity of the passive samplers. Røyset[22] found that the NILU (Norwegian Institute for Air Research) produced passive NO_2 samplers that were used in this work, were within 10%–20% of results from NO/NO_x monitors calibrated against standards, that the detection limit was one μg m^{-3} (0.5 ppb) NO_2 (7 days), that the precision was 5% and the accuracy 20%. No indoor NO_2 sources were reported in the museums or observed on inspection. The visible (lux) and UV (W m^{-2}) light levels were measured with light meters continuously (lux) in some sites, or with spot measurements mid-day (12 a.m.) each month when the sum of the (possible) natural + artificial light intensity was at its maximum and was reported as mid-day annual averages.[53] The UV wavelength band of the individual light meters could unfortunately not be verified. Light meters used in museums typically measure the UV wavelength band 300–400 nm.[54] The temperature and relative humidity (RH) were measured with the continuous loggers of the different types in regular use by the museums and reported as monthly averages.[53] The area to volume ratios of the measurement rooms and description of ventilation from the museums are given in Table 3 of the modelling results, for easier comparison with those results. The values of the light measurements are, for simplicity, given in the same Table 3.

It is important to note that the conditions in Trondheim (no. 2), Zakopane (no. 8), and partly the Malta (no. 10) museum were found to be deviating in some respects. In the Trondheim site, a chimney was observed to emit smoke from the burning of fuel oil very close to the air intake of the ventilation system on the roof. Zakopane is a much-frequented winter sports location at an elevation of ~850 m in the Tatra Mountains. In Wignacourt, the (natural) ventilation was much higher in the hot summer months, due to more opening of doors and windows, as is often the case in Malta (Cassar, J., 2005, personal communication).

TABLE 1 Museums and site descriptions

Name of museum/historic building, (U) = Urban. (R) = rural	Location, Country
1. The Museum of Decorative Arts & Design (U)	Oslo, Norway
2. Trøndelag Folk Museum (U/R)	Trondheim, Norway
3. Tower of London, Bloody Tower (U)	London, UK
4. Blickling Hall (R)	Norfolk, UK
5. Haus der Geschichte Baden-Württemberg (U)	Stuttgart, Germany
6. Schwarzwälder Trachtenmuseum (R)	Haslach, Germany
7. The Jan Matejko House (U)	Krakow, Poland
8. The Karol Szymanowski Museum "Atma" (R)	Zakopane, Poland
9. The Historical Museum of Crete (U)	Heraklion, Greece
10. Wignacourt Collegiate Museum (U/R)	Rabat, Malta

3 | RESULTS

Figure 1 shows the outdoor and indoor mean monthly concentrations of NO_2 and O_3 measured in the 10 museums.[53]

The outdoor O_3 measurement in no. 4, Blicking Hall in September (9) failed. The NO_2 outdoor concentration reported from the measurement in no. 6, Haslach in September (9) (0.6 ppb) was about one magnitude lower than in August and October. This out-layer was considered highly dubious, and without it being possible to locate the reason for the deviance, the value was removed. The NO_2 values in no. 7. The Jan Matejko House in October (8) were found to be suspicious but are reported. Figure 2 shows the NO_2 I/O ratios measured in the 10 museums. The figure also shows the result from the model fitting (See Section 4).

The figure clearly shows the higher indoor summer than winter concentrations of NO_2 measured in nine of the 10 museums and the higher than unity NO_2 I/O ratios measured in the summer in some of them. The highest summer indoor NO_2 concentrations and NO_2 I/O ratios among the 10 museums were observed in Stuttgart, excepting the special case of Trondheim (see Experimental). The indoor concentrations of NO_2 were measured to be higher than outdoors in Stuttgart from April to August. In the rural comparison, case in the

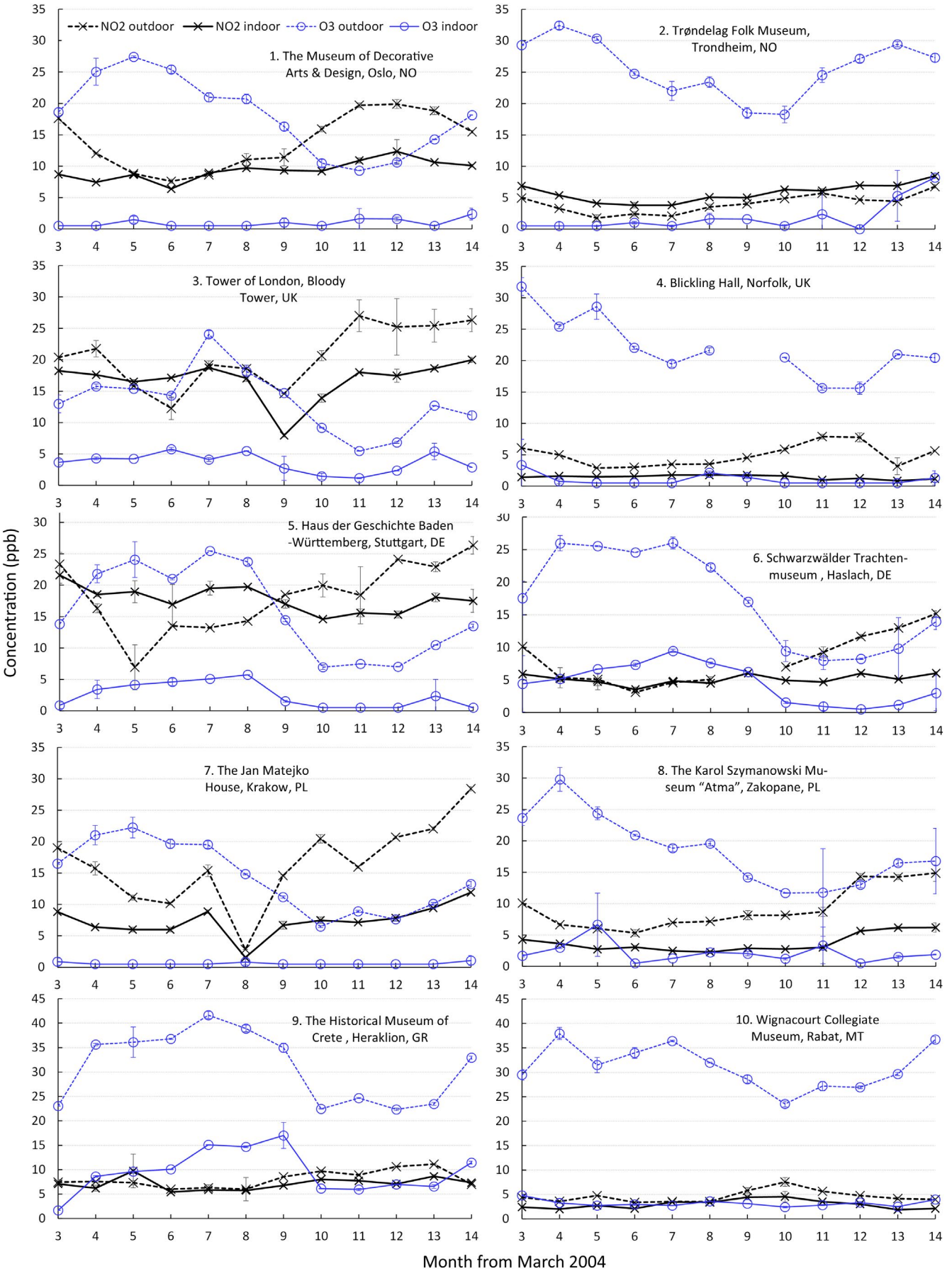

FIGURE 1 Mean monthly outdoor and indoor NO_2 and O_3 concentrations measured from March 2004 to March 2005 in 10 European museums. The error bars represent the standard deviation of duplicate measurements

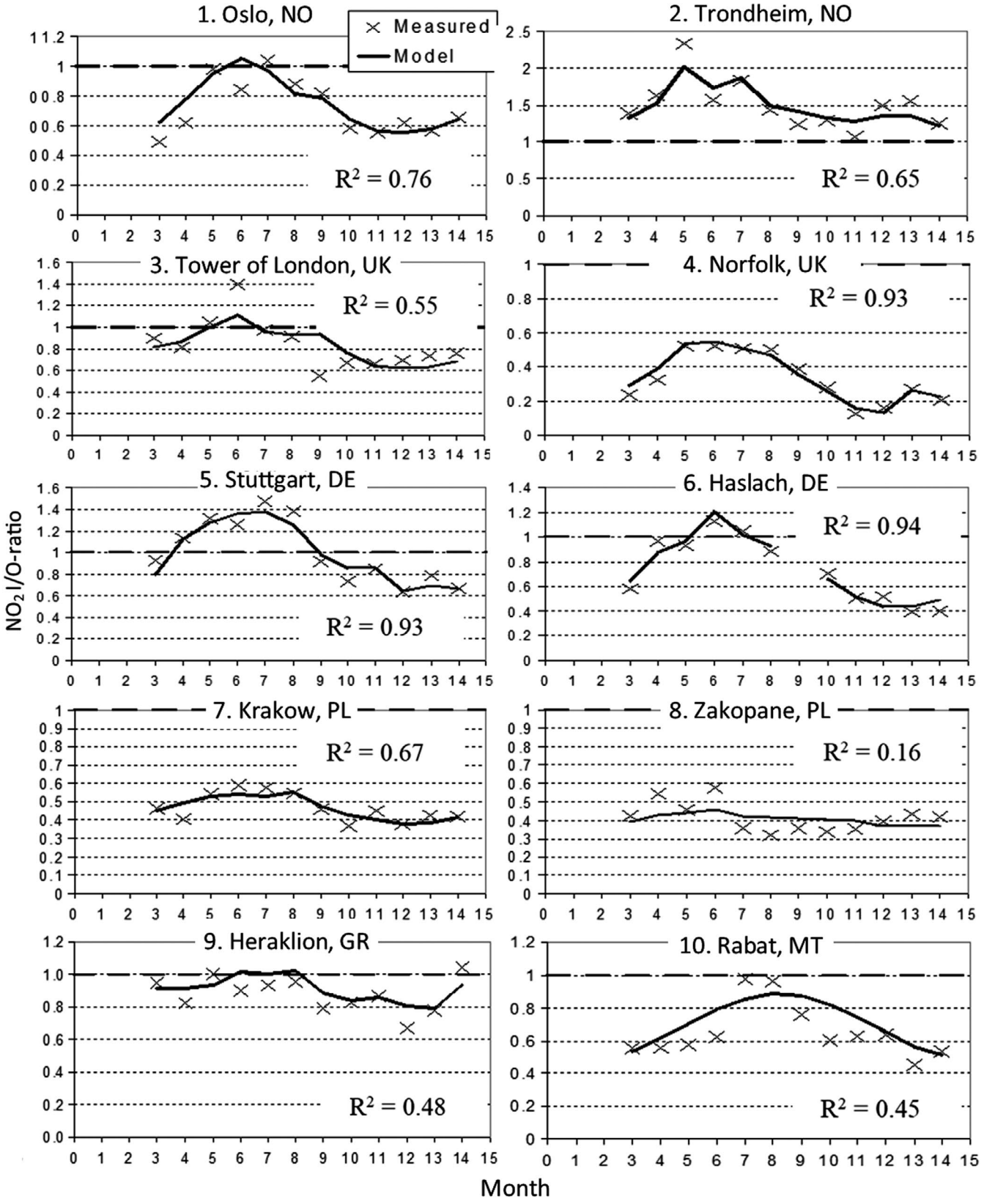

FIGURE 2 Measured and modelled monthly indoor to outdoor NO_2 I/O ratios from March 2004 to March 2005 in 10 European museums

same region (Germany), Haslach, near equal indoor and outdoor concentrations of NO_2 were observed during the summer. The observations in these two museums (nos. 5 and 6) will be discussed in some more detail together with the other sites to understand the modelling parameter fit and in the final Discussion. The annual monthly average O_3 indoor and outdoor measured values are given in Table 2.

TABLE 2 Annual average monthly O concentrations (ppb)

Site no:	1	2	3	4	5	6	7	8	9	10
O_3(i)	18.1	25.6	13.4	22.0	15.8	17.4	14.3	18.6	31.1	31.2
O_3(o)	1.0	5.7	3.6	1.0	2.5	4.5	0.6	2.2	9.5	3.2
O_3 I/O	0.05	0.22	0.27	0.05	0.16	0.26	0.04	0.12	0.31	0.10

The average annual O_3 I/O ratio over all the sites was found to be 0.16 (from Table 2).

A weak positive single parameter correlation ($ax + b$, R^2) was observed over all the sites and months for the outdoor ($a = 5$, $R^2 = 0.07$) and for the indoor ($a = 2$, $R^2 = 0.03$) monthly temperatures, and the NO_2 I/O ratio, which could be expected from the dependence of the annual variation in the NO_2 I/O ratios on the season seen in Figure 2. No significant single parameter correlations were, however, observed between the monthly outdoor or indoor temperatures or RHs and the NO_2 I/O ratios. Thus, the temperature and humidity variations seemed not to be major factors in explaining the annual variations in the NO_2 I/O ratios.

4 | MODELLING

4.1 | Model derivation and model fitting

A steady-state NO_2 I/O model that included the effect of outdoor photolysis was developed and simplified to be applied with the available mean monthly experimental measurement values. By describing (consecutive) steady states such a model will not replicate the dynamic reactivity that will be important for the concentration changes and values on short-time scales (hours). It will typically not well replicate concentration peaks or accumulated changes in long duration monotonous trends. The main influences on the NO_2 I/O ratios in a situation without indoor NO emissions can be described as follows: The higher the NO_2 ventilation from the outdoor is, and the (possible) indoor NO_2 emissions are, the higher NO_2 I/O ratios will be. The higher the deposition velocity of NO_2 to indoor surfaces (e.g.[55-58]), and the room surface area to volume (A/V) ratios, are, the lower NO_2 I/O ratios will be. In addition, one needs to consider the effects of homogeneous reactions.[10] The reversible reaction involving photolysis of NO_2, to NO and O_3 is that which mainly influences indoor NO_2 concentrations[1]:

$$NO_2 + O_2 + h\upsilon \leftrightarrow NO + O_3 \quad (1)$$

where h is Planck's constant, and υ is the frequency of light at wavelengths from 202 to 422 nm. This reaction moves toward the right outdoors, where NO_2 is split to NO and O_3 by sunlight, and to the left indoors, where there is much less light.[10,59,60]

Ozone can also react with NO_2 to generate the nitrate radical (NO_3·) which can react further to nitric acid. The second order rate constant of this reaction is, however, much slower than that of the reaction of O_3 with NO (0.0028 $ppb^{-1}\ h^{-1}$ as compared to 1.6 $ppb^{-1}\ h^{-1}$ at 25°C) and it is "not expected to greatly influence the indoor concentrations of either NO_2 or O_3."[1] Nazaroff and Weschler[1] further reported that due to the high rate of formation of NO_2 by reaction (1), NO and O_3 will usually not only be simultaneously present indoors at levels above 5 ppb, but also that the I/O ratios of NO tend to be close to unity. This is likely to be the case if near all the outdoor NO or O_3 is consumed in their rapid reaction before ventilation to the indoors. As can be the case centrally in cities with the near-total consumption of O_3 by surplus NO from traffic emissions or oppositely the near-total consumption of the remaining NO by surplus O_3 some distance away from the traffic emissions. In such situations, a typical "urban tropospheric ozone hole" is formed in the center of cities, such as for example in London.[61] The ventilation to the indoors of either O_3 or NO will then be low, and the Equation (1) equilibrium will have little influence on the indoor concentrations.

The indoor reaction of O_3 with NO is usually faster than other removal processes and thus has the potential to affect indoor concentrations, as is shown by the following examples: If an NO concentration of 5 ppb is ventilated to the indoors in the presence of O_3, the indoor removal rate of O_3 will be 7.9 h^{-1}. This is near a magnitude higher than a typical natural ventilation rate of ~1 h^{-1} and higher than that expected of the deposition of O_3 to the surfaces in a medium size room. For a typical deposition velocity of O_3 of 1.8 m h^{-1} (5 x 10^{-4} m s^{-1})[12,57,62,63] and room surface area to volume (A/V) of unity (for example a room of dimensions ≈ 10*10*3.5 m) the deposition rate would be 1.8 h^{-1}.

The reaction between NO and O_3 will, because of its high rate, typically take place in a smaller volume than the whole room and at higher concentrations of the gases than the average (measured) room concentrations (see also Section 4.3). This "problem" was avoided by deriving a model with only the outdoor concentrations as input. If mainly O_3 and NO_2 is ventilated to the indoors, then, obviously, the situation would be different with expected smaller gradients.

The model expressions for the NO_2 I/O ratio were derived based on the fundamental Equation (1), then with input from the below Equations (2), (4) and (6) that describe the rate of formation of indoor NO_2, NO, and O_3, and Equation (5) that describe the rate of formation of outdoor NO. From Equation (1) and the indoor air exchange rate with the outdoors, the change in the indoor concentration of NO_2 is given by:

$$\frac{dNO_2(i)}{dt} = \lambda \cdot NO_2(o) - \lambda \cdot NO_2(i) - \frac{A}{V} \cdot \upsilon_{d,NO2} \cdot NO_2(i) + k \cdot O_3(i) \cdot NO(i) \quad (2)$$

where $NO_2(i)$, $NO(i)$, and $O_3(i)$ are the indoor concentrations of NO_2, NO, and O_3 (ppb), NO_2(o) is the outdoor concentration of NO_2 (ppb),

$\upsilon_{d,NO2}$ is the indoor mean deposition velocity of NO_2 (m s^{-1}), k is the rate constant for the reaction of O_3 with NO (=4.43*10^{-4} ppb^{-1} s^{-1} at 25°C), λ is the air exchange rate (s^{-1}), A is the room surface area (m^2), and V is the room volume (m^3). Equation (2) assumes that there is no indoor photolysis of NO_2 to NO. Nearly all the NO_2 photolysis happens due to UV radiation (over 90% by radiation between 300 and 370 nm and not by radiation over 420 nm[60]). In line with Fiadzomor[64] and based on previous studies, Carslaw[5] reports that the attenuation of UV light from outdoor to indoor is typically about 0.03. She further refers to the modelling work of Nazaroff and Cass[6] that showed an increase in indoor from outdoor NO_2 (of 3%) when the indoor visible and UV light fluxes were 0.7% and 0.15% of outdoors. It is a general aim of museums to keep low light and especially UV levels to prevent damage to objects. The day maximum annual average visible, and UV light intensities measured in the museums of 200 lux in Blickling Hall and 15 mW m^{-2} in the Tower of London (Table 3) were about 0.3% in the winter to 1% in the summer (visible light), and 0.015% (UV light) of the outdoor radiation (of ~17 000 lux in the winter to 67 500 lux in the summer,[65] and 100 W m^{-2}[66]). This shows a similar outdoor to indoor visible light attenuation (or alternatively outdoor natural to indoor artificial light intensity) as in the modelling example from Nazaroff and Cass[6] and considerably higher outdoor to indoor UV attenuation in the museums than in that example and reported as typical in the general indoors by Carslaw.[5] At the low UV levels in the museums, there should be little indoor NO_2 photolysis, and as in the example of Nazaroff and Cass[6] an increase in the indoor to outdoor NO_2 concentration could be expected in the summer.

The following derivation assumes that there were no indoor emissions in the museums, of NO or NO_2 (that can happen from for example gas-fired stoves for heating and cooking, cellulose nitrate films or wool textiles), of O_3 (from for example photocopiers) or of terpenes or other VOC (volatile organic compounds, from for example plants, or chemical solvents) that react with O_3 at a high rate. If needed a term for indoor emissions or homogeneous production of NO_2 by another route than Equation (1) could be added to the right side of Equation (2). An expression for the NO_2 I/O ratio in the steady state was derived from Equation (2) to give:

$$\frac{NO_2(i)}{NO_2(o)} = \frac{\lambda + \left[kO_3 \cdot (i) \cdot NO(i)\right]/NO_2(o)}{\lambda + \frac{A}{V} v_{d,NO2}} \quad (3)$$

The interest was now to obtain an expression for the NO_2 I/O ratio with the outdoor pollution (the outdoor concentrations of NO_2 and O_3, and the outdoor emission rate of NO) and indoor building parameters (the room volume and surface area, and the deposition velocities of NO_2 and O_3 to the room surfaces) as input. This was achieved by the following derivation of expressions for $O_3(i)$ and NO(i) from these parameters, to be input in Equation (3).

The change in the concentration of NO in the indoor air was calculated as:

$$\frac{dNO(i)}{dt} = \lambda \cdot NO(o) - \lambda \cdot NO(i) - k \cdot O_3(i) \cdot NO(i) \quad (4)$$

where NO(o) is the outdoor concentration of NO (ppb). The indoor deposition velocity of NO was set to 0.[1,4] In the absence of NO data, as input for NO(o) in the steady-state solution of Equation (4) (see Equation (7) below), the change in the concentration of NO in outdoor air was calculated as:

$$\frac{dNO(o)}{dt} = -k \cdot O_3(o) \cdot NO(o) + j \cdot NO_2(o) + e \quad (5)$$

where O_3(o) is the outdoor concentration of O_3 (ppb), j is the photolysis rate constant for NO_2 (s^{-1}), and e is the outdoor emission rate of NO (ppb s^{-1}). Finally, the change in the concentration of O_3 in indoor air was calculated as:

$$\frac{dO_3(i)}{dt} = \lambda \cdot O_3(o) - \lambda \cdot O_3(i) - k \cdot O_3(i) \cdot NO(i) - \frac{A}{V} \cdot v_{d,O_3} \cdot O_3(i) \quad (6)$$

where υ_d (O_3) is the indoor mean deposition velocity of O_3 (m s^{-1}). For a steady-state situation, NO(i), NO(o), and O_3(i) were then calculated from Equations (4), (5), and (6) to give, respectively, Equations (7), (8), and (9):

$$NO(i) = \frac{\lambda}{\lambda + k \cdot O_3(i)} NO(o) \quad (7)$$

$$NO(o) = \frac{j \cdot NO_2(o) + e}{k \cdot O_3(o)} \quad (8)$$

$$O_3(i) = \frac{\lambda \cdot O_3(o)}{\lambda + k \cdot NO(i) + \frac{A}{V} \cdot v_{d,O3}} \quad (9)$$

A new expression for NO(i) was then obtained by substituting NO(o) and O_3(i) in Equation (7) with the expressions for these parameters given by Equations (8) and (9), and then solve as a second order polynomial to obtain:

$$NO(i) = \frac{-B + \left(B^2 - 4AC\right)^{-0.5}}{2A} \quad (10)$$

with

$$A = k \cdot \lambda \quad (11)$$

$$B = \lambda^2 + k \cdot \lambda \cdot O_3(o) + \lambda \cdot v_{d,O_3} \cdot \frac{A}{V} - \lambda\left(\frac{j \cdot NO_2(o) + e}{O_3(o)}\right) \quad (12)$$

$$C = \left(\lambda^2 + \lambda \cdot v_{d,O_3} \cdot \frac{A}{V}\right)\left(\frac{j \cdot NO_2(o) + e}{k \cdot O_3(o)}\right) \quad (13)$$

The expression for O_3(i) given by Equation (9) and that for NO(i) given by Equations (10) to (13), were then inserted for these parameters in Equation (3) to obtain the needed expression for the NO_2 I/O ratio. The outdoor emission rate of NO, e, given as concentration per time unit, was interpreted here as the contribution

TABLE 3 The model, Equation (14) best fitting parameter values in the 10 European museums

	Measurements			Parameter boundaries					
				Min = 0.1, max = 10		Min = 0, max= 0.01	Min = 0, max = 0.25	Min = 0, max = 1	Combined evaluation parameter
				Model parameters					
Site no.	Visible light (Lux)	UV (W m^{-2})	Room A/V (m^{-1})	λ (h^{-1}), modelled ventilation	λ (h^{-1}), description from museums	v_dNO_2 (m s^{-1})	e (ppb s^{-1})	x	$(e\ x\ x^2)/(A/V\ x\ v_dNO_2)$
1	2.0	0	1.0	1.5	Natural	0.0011	0.25	0.18	7.4
2	0.4	0	0.5	10	~4 h^{-1} during opening hours	0.00036	0.25	0.15	**31**
3	120	15	0.6	2.2	Natural, very considerable	0.0016	0.040	0.45	**3.9**
4	200	5	0.8	0.28	Natural, barely noticeable to noticeable	0.0092	0.0053	0.96	0.67
5	21	0	0.5	0.10	Barely noticeable	0.010	0.25	0.58	**17**
6	6.5	0	3.6	0.82	Barely to easily noticeable	0.00023	0.010	0.42	2.1
7	16	0.1	1.1	6.8	Natural	0.0032	0.0026	0.61	0.27
8	12	0	1.5	6.8	Natural	0.0028	0.25	0.13	1.0
9	140	0.7	1.3	9.4	Mechanical	0.0021	0.25	0.25	**5.7**
10	23	3	1.1	0.12	Natural, very still air	0.000091	0	0.16	0

Note: The hatched horizontal lines distinguish between the two museums in each of the five European regions. The bold figures represent the highest combined evaluation parameter value of the two museums in each region. A ranking seemed not meaningful between Krakow (no. 7) and Zakopane (no. 8) due to the low R^2 in Zakopane (Figure 2).

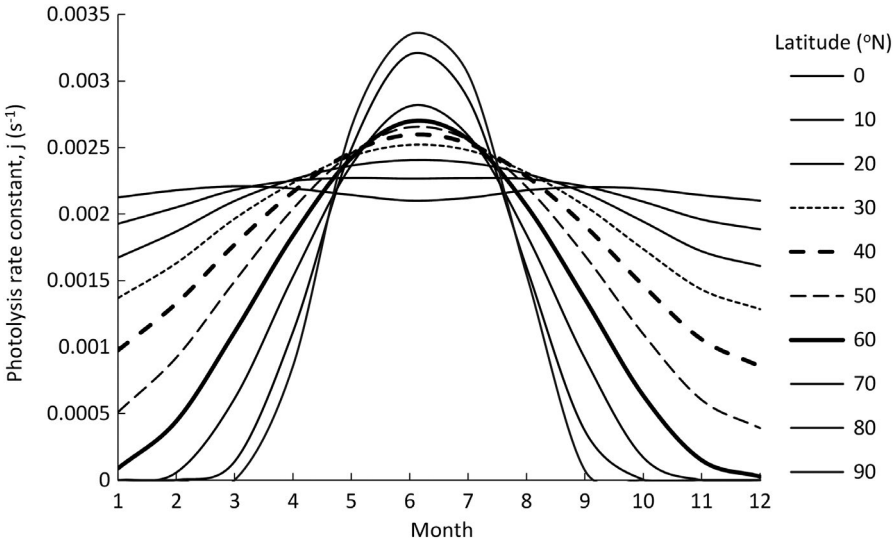

FIGURE 3 Mean monthly photolysis rate constant for the outdoors splitting of the NO_2 molecule dependent on month and latitude, at 50% cloud cover

of outdoor emissions of NO to the concentration of NO at the air intake to the building. In the modelling, the NO emission rate was set to be constant through the year and contribute to the varying outdoor NO concentrations by Equation (8). It was beyond this work to collect traffic counts representative for the emissions at the study sites. However, some reports show little monthly variations in Europe. Statistical evaluations from Poland[67] showed that month of the year was of little importance in explaining seasonal road traffic variations. Measurements of real-time traffic flows in Athens, Greece from 1997 to 1999 showed no monthly variation in 10 months, but somewhat lower counts in July and August[68] (see also Discussion). In other modelling cases, it may be more practical to use NO concentrations, from for example measurements, as input directly, and thus simply substitute Equation (8) and the similar last terms in Equation (12) and (13) with "NO(*o*)."

A model simplification was then derived to be used with the available monthly mean values for the outdoor concentrations of NO_2. Instead of the, supposedly more physically correct, derivation of NO(*i*) and O_3(*i*) described above as input in Equation (3), the I/O concentrations of NO and O_3 (NO(*i*)/NO(*o*) and O_3(*i*)/O_3(*o*)) were in the simplification assumed to be a fraction, *x*, being present in a steady state through the year. The value of this fraction should be interpreted as the root product $(x_1 \times x_2)^{0.5}$ of the average annual I/O ratio x_1 of O_3 and x_2 of NO. From the literature, it seems that the I/O ratio of O_3 is commonly about 0.5[19] and of NO closer to 1,[1] which would give a single parameter value of $x = 0.7$. The overall annual average O_3 I/O ratio measured at the sites in this work was 0.16 (Table 2), which would with an NO I/O ratio of 1 give a value of $x = 0.4$. With reaction of NO indoors to an NO I/O ratio < 1, *x* would be lower. By multiplying Equation (8) with $k \times O_3(o)$ and then dividing the numerator and denominator of the fraction in the numerator of Equation (3) ($[kO_3(i) \times NO(i)]/NO_2(o)$), with respectively, the left and right side of this developed Equation (8), and then substituting for the NO I/O- and O_3 I/O-concentration fractions their assumed equal ratios, *x*, the model simplification was obtained as:

$$\frac{NO_2(i)}{NO_2(o)} = \frac{\lambda + x^2 \cdot \left(j + \frac{e}{NO_2(o)}\right)}{\lambda + \frac{A}{V} \cdot v_{d,NO_2}} \quad (14)$$

The temperature-dependent NO + O_3 rate constant, *k* (Equation (2)), does not appear in Equation (14). The temperature dependence of the NO_2 photolysis rate is slight in the ambient temperature ranges of the 10 museums.[60] If the emission rate, *e*, in the Equation (14) is expressed by calculation from Equation (8), then Equation (14) is equal to Equation (3), only with $xO_3(o)$ and $xNO(o)$ substituted for $O_3(i)$ and NO(*i*) in Equation (3). This simple formula, Equation (14), had the advantage that there was no need for measured values for, or complicated modelling of, the indoor concentrations of O_3. The procedure for the calculation of the photolysis rate, *j*, of NO_2, was adopted from the EMEP Unified model[69,70]:(22). The calculation was made from the general expressions, and coefficients for the NO_2 photolysis, in[70]:(22) for every day and hour of the year for each 10th degree of latitude from the Equator (0°) to the North Pole (90°). A cloud cover of 50% through the year was used for all the sites except Malta and Crete where a cloud cover of 30% was used, based on rough annual averages[71-73]. Figure 3 shows the latitude-dependent mean monthly averaged values for the photolysis rate constant for the O_3 + NO reaction, with 50% cloud cover, that can be used as input in Equations (14), and (15), to avoid lengthy calculations of this.

From Equation (14), it can be observed that for a case when the outdoor photolysis of NO_2 is the only source of indoor NO, and there is thus no ventilation from outdoor of directly emitted NO ($e = 0$), or indoor direct emissions of NO, then the concentration of NO_2 indoors can still be larger than outdoors. This will be the case when the indoor formation rate of NO_2 from NO and O_3 (by Equation (1) and given in Equation (14) as the multiple of the indoor to outdoor fractions of NO and O_3 and the photolysis rate, x^2j), is larger than its deposition rate to the indoor surfaces ($A/V \times v_{d,NO2}$). Thus, the chance for an NO_2 I/O ratio > 1 increases in the summer, except close to the equator, and more so at higher latitudes (Figure 3).

The model fitting to the annual NO_2 I/O values at the 10 museums was performed with Equation (14) and was shown in Figure 2 with the experimental measurements. Mean monthly outdoor NO_2 concentrations and the calculated mean monthly photolysis rates in a situation with 50% cloud cover (from Figure 3), or 30% cloud cover for the sites in Crete (No. 9) and Malta (No. 10), were used. The other parameters in Equation (14) were assumed constant throughout the year and their values found from the modelling. Maximum and minimum allowed model parameter boundary values (Table 3) were set to avoid modelling to unreasonable continuously increasing values with infinitesimal improvement in the fitting. The low boundary was set to zero, or to a "low" value where this was needed to obtain a result from Equation 14 (of the ventilation rate, Table 3). The high boundary was set to a value in the high range of what was thought realistic for any site, compared to reported values. Thus, it was assumed that a ventilation rate above 10 h^{-1}, a deposition velocity of NO_2 above 0.01 m s^{-1},[57] and an NO emission rate (e) over 0.25 to be unrealistic (Table 3). e = 0.25 represents a mean monthly NO concentration of 34 ppb by Equation (8) when assuming a photolysis rate of 0.0026 (Figure 4), or of 47 ppb mid-summer (July 1st) in Madrid, Spain (see below), and equal NO_2 and O_3 concentrations of 20 ppb. The model fitting was performed with a least-squares multiple parameter nonlinear regression method in SPSS[1]. The parameter values were from the start of the manual modelling procedure set to the mid-point within their boundary ranges (see Table 3). The parameter values were then changed, consecutively between the parameters, and iteratively one small step at a time, until the apparent best possible fit and R^2 was achieved. The procedure was repeated several times with some changing of the start values and orders of change in values of the parameters, to be confident about the solutions. In practice, the optimal (largest possible) R^2 was typically obtained by doing a few (3–4) initial rounds of iterations with initial larger changes in the parameter values to investigate the sensitivity, then with fine tuning with minor changes to obtain the maximum R^2.

Figure 2 shows that Equation (14) could reasonably simulate the annual variation in the NO_2 I/O ratio, except in Zakopane where the R^2 was low. The model fit was quite close for Blickling Hall in Norfolk, UK (no. 4) and the two German museums in Stuttgart and Haslach (nos. 5 and 6). Table 3 gives the parameter values from the modelling.

Although the results from the manual iterations seemed convincing in finding the best possible fits, it was realized that this method might not guarantee the testing of all possible parameter value combinations and full randomization of the input. With the four independent variables (λ, v_{dNO2}, e, and x) combined in Equation (14) and, additionally the ill-defined A/V ratios it was suspected that the modelling might not result in parameter values that could be simply explained by the observed site characteristics (Table S1 and Table 3). It was expected that interpretation by the combined equation parameters: x^2 x e, describing the contribution of the outdoor emission of NO and the I/O ratios of NO and O_3 to the indoor NO_2, and A/V x v_{dNO2} describing the heterogeneous indoor removal of NO_2, might be more realistic, although it would give less specific information. This is not so surprising as the (non-measured) individual independent parameters are in direct combination in Equation (14), and thus not clearly distinguishable in the modelling, and also, as this combined parameter start to resemble the full model expression in Equation (14). It can be observed in Table 3 that the combined parameter distinguishes roughly between the urban and more polluted sites, and rural and less polluted sites.

4.2 | Model evaluation and sensitivity

The expression for the A/V ratio giving an NO_2 I/O ratio equal to 1 can be derived from Equation (14) to be:

$$\frac{A}{V} = \frac{x^2\left(j + \frac{e}{NO_{2(o)}}\right)}{v_{d,NO_2}} \quad (15)$$

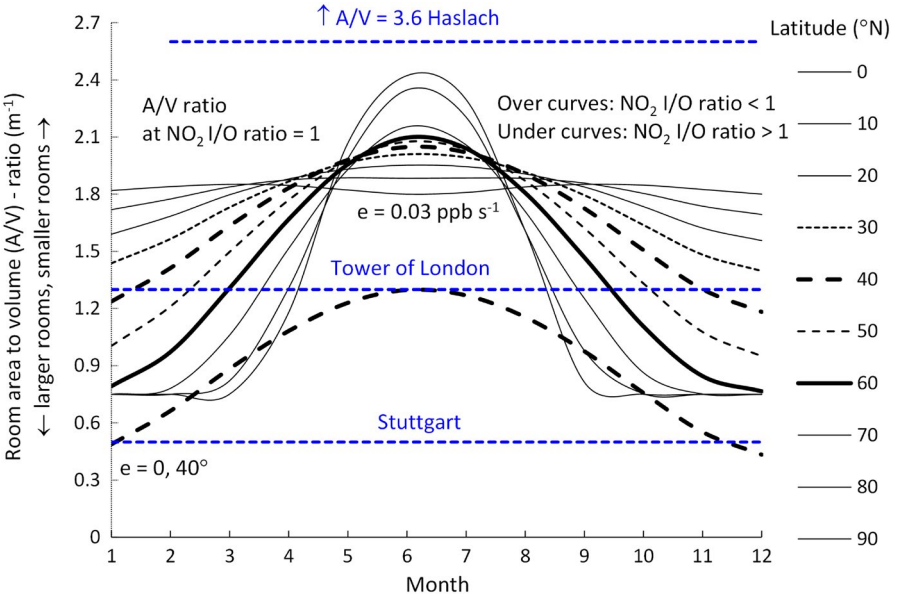

FIGURE 4 Room size, given by the room surface area to volume (A/V) where an NO_2 I/O ratio = 1 is expected, without (e = 0, as a reference at latitude 40°N) and with (e = 0.03 ppb s^{-1}) close to the building outdoor NO emissions, depending on month of the year and latitude. ($NO_2(o)$ = 20 ppb, $v_{d,NO2}$ = 5 x 10^{-4} m s^{-1}, x = 0.5). The room A/V ratios in some of the museums are given

Figure 4 shows the room sizes, given by the room surface area to volume (A/V) from Equation (15), where an NO_2 I/O ratio of unity is expected, depending on the month of the year and latitude, as given by the mean monthly photolysis rates of NO_2, j, with a 50% cloud cover from Figure 3 and with outdoor NO emissions, e, of 0.03 ppb s^{-1} close to the building air intake. With an NO emission rate of 0.03 ppb s^{-1} the outdoor mean monthly NO concentration would, by Equation (8) and assuming equal NO_2 and O_3 concentrations of 20 ppb, be about 10 ppb in the summer, but varying with the photolysis rate through the year and depending on latitude, from 3.4 to 11 ppb. A mean annual average NO_2 of 20 ppb was measured at the 10 museums. O_3 concentrations can typically be below 20 ppb in city centers and above 20 ppb away from traffic emissions ([61]). NO concentrations from 3.4 to 11 ppb represent typical annual measurements at stations in Europe.[24] The NO_2 deposition velocity to the indoor surfaces was set to 5 x 10^{-4} m s^{-1},[57] and the multiple of the I/O ratios of NO and O_3 (x^2) to 0.25 ($x = 0.5$) like the mean of the modelling results in Table 3 when excluding the deviating sites, no 2, 8, and 10 (see Experimental and sites), which is in the range of reported values and complemented with the O_3 measurements in this work (see Modelling).

Rooms positioned under the curves in Figure 4, that is, with a smaller A/V ratio and thus being larger, are expected to have NO_2 I/O ratios larger than unity. As A/V ratios are usually, due to the roughness of room surfaces, furniture, installations, and other features, larger than those calculated from the nominal room dimensions, rooms usually need to be larger than indicated by the nominal A/V ratios for NO_2 I/O ratios above unity to be observed. Indoor deposition velocities are expected to vary more than one magnitude depending on the surface material, humidity, and temperature.[57] An NO_2 deposition velocity of 5 x 10^{-4} m s^{-1} is in the upper range of values measured for common room surface materials in the laboratory,[57] and could include some measure of the effect of the typical more complex room features. As a an example, for a case as described by Figure 4 at 40°N (that could be in Madrid, Spain), and with an outdoor NO emission of 0.03 ppb s^{-1}, it could be expected that mid-summer, as an average for June and July, then for rooms with A/V ratios less than ~2 m^{-1} (i.e., of, unfurnished, dimensions larger than about 4 x 4 x 2 m) the indoor concentration of NO_2 will be larger than the outdoor concentration. Around July 1st the photolysis rate would be at its largest in Madrid: $j = 8.14*10^{-3}$ s^{-1}.[60] A larger indoor than outdoor concentration is then expected in volumes larger than 1.2 m^3, and thus in practice nearly always. In other seasons the rooms would need to be larger for the NO_2 I/O ratio to be above unity at the elsewise same conditions. With a higher photolysis rate than in Madrid, which could be expected further north in the summer or further south in the other seasons, and elsewise similar conditions as laid out above, higher NO_2 I/O ratios could be expected in smaller rooms than in the Madrid example. With increasing infiltration of NO and O_3 (to $x > 0.5$) the sizes of rooms where an NO_2 I/O ratio above unity is expected is decreasing even more quickly, to an extent that the infiltration becomes relatively more important for the NO_2 I/O ratio than the latitude or time of year (see Figure S1).

From the room A/V ratios (Figure 4) a much larger difference in the NO_2 I/O ratios between the Stuttgart and Haslach sites than observed in Figure 2 might be expected, with ratios always above unity in Stuttgart and never above unity in Haslach. In comparison for three of the locations with an A/V ratio of between 1 and 1.5 (no. 3, Tower of London in Figure 4, and nos. 1 and 9 (Table 3), the prediction from Equation (14) of NO_2 I/O ratios above unity in the summer (Figure 2) seems reasonably correct. Possible reasons for the smaller measured than modelled difference in the NO_2 I/O ratio between the Stuttgart and Haslach sites can be evaluated through the model (Equation (14)) sensitivity to the input parameters. Figure 5 shows the change in the NO_2 I/O ratios at the three sites (Stuttgart, Tower of London, and Haslach) estimated to happen by changing the value of each model parameter (Equation (14)) from those measured in June 2004 (the crossing points of each parameter curve with the horizontal line for the NO_2 I/O ratios).

Figure 5 shows the negative influence on the NO_2 I/O ratio of the indoor deposition velocity $\upsilon_d(NO_2)$, of smaller rooms (higher A/V) and of the outdoor NO_2 concentration, and a positive influence of the other parameters. The NO_2 I/O ratio is at all the three sites most sensitive to changes in the indoor deposition velocity with a somewhat different ranking of the sensitivities to the parameters between the sites. The figure shows that the measured or most likely separate site deviances from the average modelling conditions, used in Figure 4, would reduce the difference in the I/O ratio between the sites observed in that figure: It may be that the deposition of NO_2 in the mechanical ventilation system and through the modern building shell in Stuttgart was higher than the average value used in the modelling, which was also indicated by the high modelling results of the deposition velocity in Stuttgart (Table 3); the outdoor NO_2 concentrations in Haslach were considerably lower (~5 ppb, Figure 1) than the used museums average of 20 ppb; and the larger complex of interconnected rooms in the Haslach museum may have had a lower effective A/V ratio then 3.6. A change in these directions along the parameter curves in Figure 5 (as visualized with the arrows) would reduce the NO_2 I/O ratio in Stuttgart and increase it in Haslach, and thus work in the direction of the measurements (as compared to the modelling in Figure 4).

4.3 | Limitation of the model and available data

It should be stressed that the steady-state model presented in this paper does not include homogeneous reactions of NO_x with other species (than O_3), that were not measured but may have been present and had an influence on the NO_x values. The reported monthly averaged data do not describe variations in the indoor concentrations of NO_x and O_3 due to the dynamic reaction between them. For that purpose, time-dependent analytical solutions or, more reasonably, numerical modelling to much more time resolved concentration data (<hourly) would be needed. How well the presented steady-state box modelling would describe data with a different, for example, from hourly to monthly, time resolution is a question of

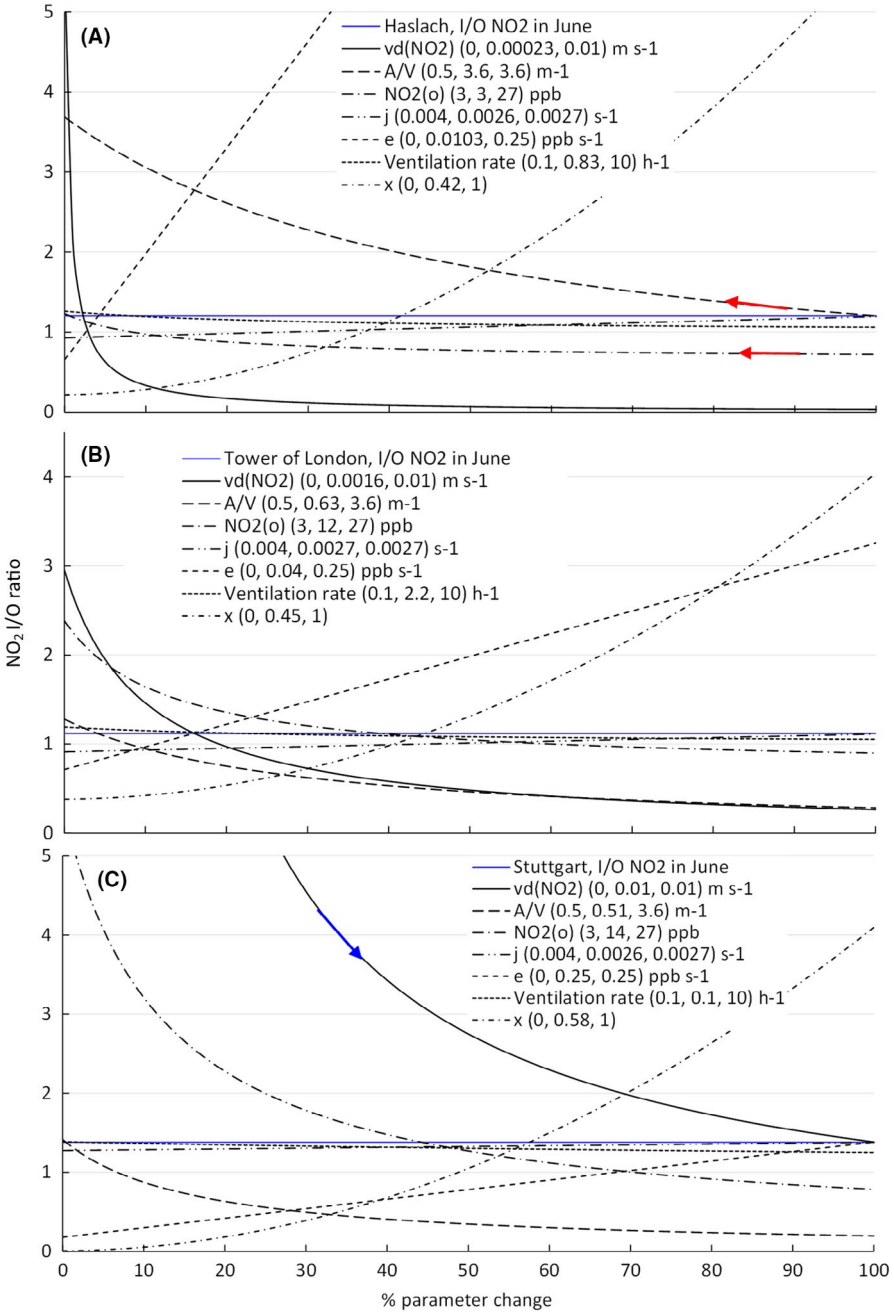

FIGURE 5 Sensitivity of the modelled June 2004 NO_2 I/O ratios (by Equation (14)) to the input parameters in (A) Haslach, (B) Tower of London, and (C) Stuttgart. The three values in the brackets are the minimum (0%), the measured values at the sites that were kept constant when varying the other parameters, and maximum values (100%) in the modelling ranges over all the sites (nos. 1 to 10, Table 3), but in the monthly mean variation of *j* at the latitude (50° north) of the three sites, and in the $NO_2(o)$ concentration measured over the three sites (Figure 1). The arrows indicate the measured or likely direction of changes in the given parameter values and resulting NO_2 I/O ratios from the average model values used in the calculations of the curves in Figure 4, for the Stuttgart and Haslach museums (according to Figure 1, $NO_2(o)$, and Table 3, A/V and v_dNO_2)

interest. The parameter values that could be obtained from fitting of time–dependent dynamic models to data with higher time resolution could be different from those obtained in this work and could be expected to be more physically correct.

There is, typically, large fluctuations in the diurnal concentrations of NO_x and ground level O_3, especially due to traffic emission cycles.[74] The variations in the outdoor concentrations and rapid reaction between NO and O_3 implies that homogeneous mixing of O_3 and NO will seldom happen in rooms after ventilation to the indoors. Gradients in the indoor concentrations of the gases are expected from inlets to outlets and depending on the air flows and mixing situations. In low ventilation situations, the reaction of O_3 with NO could go to completion close to the inflow of air into a room but depending on the UV light presence and NO_2 photolysis. The reaction may thus happen in smaller volumes, than the total rooms, and at higher than measured mean indoor room concentrations. This might affect reaction rates and the NO_2 I/O ratios in ways that were not captured by the performed modelling.

Four independent model parameters were not measured and are interdependent (more or less) in the model expression. This situation was expected to result in considerable uncertainty, and there may have been a risk for "overfitting" and obtaining too high explanatory power (R^2). Parameter value boundaries were set in the modelling to avoid this. The main reason for the model fit (R^2) to the annual trends in Figure 2, seemed to be the similar shape through the year of the curve of the NO_2 photolysis rate as the NO_2 I/O ratios. Fitting to the variations over the year (from the smooth change in the annual trend of the photolysis rate) was then obtained, to a larger or lesser

degree, by varying the other model parameters. Resulting in clearly differing model fit between the museums. Without measured values for these properties in the museums (Table 3) that could be used as input and/or verification, caution was needed in the interpretation of their model values. Much of the experimental variation that could not be explained by the modelling (excluding effects of experimental uncertainty) might be explained by variations through the year in the assumed constant model parameters. Despite such imprecisions, the results seem to substantiate the, often, dominating effect of the outdoor NO_2 photolysis in giving systematic annual variations in the NO_2 I/O ratios with higher values in the summer. This seemed to be the case in nine of the 10 investigated museums.

5 | DISCUSSION

In all the museums except in Zakopane, higher NO_2 I/O ratios were measured in the summer than winter, corresponding with the higher outdoor photolysis rates in the summer and thus supporting the hypothesis that the difference in the outdoor to indoor photolysis rate of NO_2 was a main reason for the observed monthly variations in the I/O NO_2 ratios over the year. The lower than unity NO_2 I/O ratios measured through the year in four of the 10 locations (nos. 4, 7, 8, and 10) indicate relatively larger indoor NO_2 sinks and/or lower ventilation to the indoors of NO_2, by the precursors NO and O_3 in these than the other locations. In Trondheim (no. 2), it seemed that more NO_2 from the close to the air intake chimney emissions were measured indoors than at the outdoors location, which was positioned at some distance from the chimney and lower down on a wall, and that this could explain the high NO_2 I/O ratios > 1 in the winter. The comparison of the indoor and outdoor NO_2 and O_3 concentrations measured in Stuttgart (no. 5) and Haslach (no. 6; Figures 1 and 2) illustrate differences between a modern museum centrally located in a city, close to roads with expected significant NO traffic emissions, and a more traditional building in a rural location. A reason for the lower indoor O_3 and higher NO_2 I/O values in Stuttgart than Haslach in the summer seemed to be the higher NO outdoor emissions in Stuttgart and homogeneous NO_x-O_3 chemistry. The NO_2 concentrations were measured to be considerably higher in Stuttgart than Haslach, and the modelling results (Table 3) supported the expectation of higher outdoor NO emissions in Stuttgart. In the winter, the NO_2 concentration was considerably higher outdoors than indoors at both sites. In the summer, the opposite situation, with considerably higher indoor than outdoor concentrations, was measured in Stuttgart whereas in Haslach the outdoor and indoor NO_2 concentrations were found to be near similar. In Stuttgart more than Haslach, and especially in the summer, the indoor NO_2 concentration followed the (pattern of the) variation in the outdoor O_3 rather than outdoor NO_2 concentrations, which indicates formation of NO_2 indoor from O_3 and NO by Equation (1). In Haslach the indoor NO_2 followed the values and variations of the outdoor NO_2, but with lower indoor than outdoor values in the winter months with expected less ventilation. In Stuttgart the indoor NO_2 did not follow the values and variations

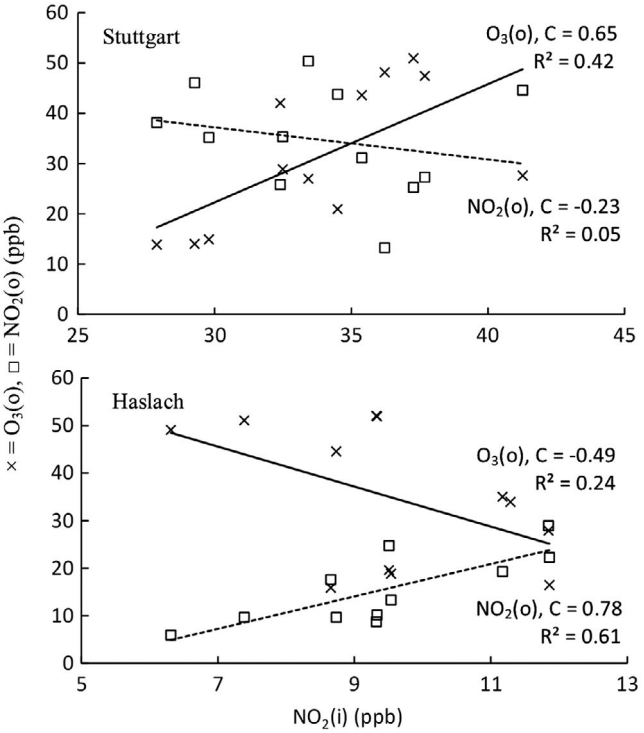

FIGURE 6 Correlation coefficient (C) and linear trend explanatory power (R^2) of the monthly averages of NO_2 measured indoors (i) with those of NO_2 and O_3 measured outdoors (o) through the year in Stuttgart and Haslach

of the outdoor NO_2. This is clearly seen in the correlation diagrams for all the months of the year in Figure 6.

The higher outdoor and, more so, indoor O_3 concentration in Haslach than Stuttgart from February to September support the hypothesis of more indoor O_3 loss in Stuttgart than Haslach due to reaction with NO. It was speculated that some infiltration through a near window, which the museum however informed was always kept closed, might have contributed to the relatively higher O_3 indoor values in Haslach.

The *emission rates of NO* were found in the modelling (Table 3) to be larger in three of the five regional urban than more rural sites. The two exceptions being the urban sites of Oslo (no. 1) and Krakow (no. 7), as compared to the smaller towns of Trondheim (no. 2) and Zakopane (no. 8; Table 3) both with, seemingly, special emission conditions, as was explained above. The literature[68] indicated that road traffic counts, and then probably NO emissions, might in some cases be lower in the summer vacation months (July and August) than other months of the year. If this was the case at the museum sites it would imply less outdoor (Equation (5)) and then indoor (Equation (4)) NO, a lower NO_2 I/O ratio (Equation (14) and Figure 6) in the summer, and an expected worse model fit. At the winter sports location of Zakopane, especially, it could be hypothesized that this was a factor. Lower NO_2 I/O values were observed in Zakopane from July to November, contrary to the model expectations, giving the worst model fit among the museums. A meaningful comparison of the modelling results for the two Polish sites was thus

difficult. One could speculate that during the colder winter than in Krakow, and with the winter sports activities in Zakopane, there was also relatively more NO emissions from solid fuel burning, of coal and wood, and/or from traffic emissions in the winter than summer in Zakopane than Krakow, that reacted indoors with O_3 to NO_2.

Unfortunately, measurements of the building and/or room *ventilation rates* were not generally available from the sites. The qualitative descriptions of the ventilation, and in one case (Trondheim) a quantification (Table 3), seemed to be in rough accordance with the values obtained from the modelling. A much higher natural ventilation in the Wignacourt Collegiate Museum in Malta in the summer than winter (see Experimental) probably explained the high values of the NO_2 I/O ratio in July and August that the model could not be fit very well. The modelling gave a similar spread in the *deposition velocity of* NO_2 between the museums, as has been measured in the laboratory (~two orders of magnitude), but with an average value about six times higher, 0.003 m s^{-1} as compared to 5 x 10^{-4} m s^{-1}.[57] The measurement data were not sufficient to explain the high values and differences between museums. They might be due to the modelling to a situation with the nominal (smaller than real) room areas, and possibly due to additional deposition happening along the infiltration path of the inflowing air in the museums, through the building shell and in ducts, and in adjoining rooms. It could be suggested that the low deposition velocity in the Wignacourt Collegiate Museum in Malta (no. 10) was related to low ventilation and air flows at that site. The model values of the NO and O_3 I/O ratios, "*x*" in Equation (14), showed a wide variation between 0 and 1 (Table 3). The mean of $x = 0.5$ (when excluding the deviating sites, no 2, 8, and 10, see above) seems reasonable, but the data seemed insufficient to explain the variation between the sites.

6 | CONCLUSION

The photolysis of NO_2 outdoors and back-reaction of NO and O_3 to NO_2 indoors can result in higher than unity NO_2 I/O ratios in rooms that are sufficiently large for this production to by higher than the heterogeneous loss by surface deposition. This can happen especially on sunny summer days, in urban areas with high NO emissions. The measurements in 10 European museums clearly showed higher NO_2 I/O ratios in the summer than winter and in the urban than more rural sites. A steady-state model of the NO_2 I/O ratio, including the photolysis effect and main indoor sources and sinks of NO_2 were derived. With a fractional (x) reduction in O_3 and NO from the outdoors to the indoors, a reasonable fit to the yearly trend of monthly mean NO_2 I/O ratios was obtained in nine of the 10 museums. The model can be used to approximate (with considerable uncertainty) indoor from outdoor NO_2 mean monthly concentrations and exposure doses that could be compared with recommended levels in museums. It is suggested that the model (Equation (14)) could, generally when other specific information is not available, be used with the average values of $x = 0.5$, $\upsilon_d(NO_2) \approx 0.003$ m s^{-1} found from the modelling of the sites in this work and with nominal room surface areas. The location-dependent mean monthly photolysis rate, *j*, at 50% cloud cover could be read from Figure 3. The emission rate of NO which is needed for the estimation can be found from the close to the building outdoor concentrations of NO_2, O_3, and NO (by Equation (8)). For outdoor concentrations of NO_2 and O_3 of 20 ppb, and a summer value of NO in Europe of about10 ppb, a value of the emission of NO of 0.03 ppb s^{-1} can be used. The model could in practice provide sufficiently good indications of high indoors, and in the summer sometimes higher than outdoors, NO_2 values that would be a preventive conservation concern. The model and its sensitivity analysis might be equally useful as a tutorial. Measurements are still recommended to obtain certain site values. The photolysis part of the modelling could possibly be added to available I/O gaseous pollution estimation tools for cultural heritage, such as IMPACT.[75,76] Such integration may be needed for the model to be practically applicable in most situations.

ACKNOWLEDGMENTS

The author wants to thank the NILU-Norwegian Institute for Air Research EU FP5 Master (EVK-CT-2002-00093) project leader Elin Dahlin, and senior researcher at NILU Jan F. Henriksen, for the initiation of the Master project. Without them the extensive environmental data base from the European museums that was the basis for this work would not have existed. A similar great thanks to the Master project partners without whose dedicated participation this work could not at have later been carried out: Mihalis Lazaridis at the Technical University of Crete, Department of Environmental Engineering in Chania, Crete, Greece; Janusz Czop at the National Museum of Krakow in Poland, Anne Sommer-Larsen at the Trøndelag Folk Museum in Trondheim, Norway, Kathryn Hallett at Historic Royal Palaces in London, UK; Christopher Calnan at the National Trust, Bury St. Edmunds, UK; Christoph Pitzen at the Württembergisches Landesmuseum Landesstelle für Museumsbetreuung Baden Württemberg, Stuttgart, Germany; and JoAnn Cassar at the Institute for Masonry and Construction Research, University of Malta in Msida, Malta. The author further wants to express gratitude to the many other people who were involved in the planning and carrying out of the Master project: May Cassar, Nigel Blades and Joel Taylor at the University College of London, and Jürgen Heinze, Sara Rentmeister and Michael Hanko at the Albert-Ludwigs-Universität, Freiburg, who gave important input. Martin Schwendemann for his participation on behalf of the Schwarzwälder Trachtenmuseum in Haslach, Germany, and Mgr. John Azzopardi for his participating support at the Wignacourt museum in Malta. Thor Ofstad who did important laboratory work at NILU. Sissel Myhrvold at The Museum of Decorative Arts and Design in Oslo, Sander Solnes at the Trøndelag Folk Museum, Louis Ayres at Blickling Hall, Norfolk, David Howell at The Tower of London, Alois Kraftczyk at the Schwarzwälder Trachtenmuseum, Pawel Karaszkiewicz and Michal Obarzanowski working for the National Museum in Krakow, and Thodoros Glytsos from the Technical University of Crete who were responsible for invaluable

sampling, measurements, registration, and reporting from the Museums. Without their efforts to make the Master Field test a success this paper could not have been written. This work was funded by the European Commission as a part of the 5th FP, Key Action, Cultural Heritage and City of Tomorrow, and by a significant grant from the Norwegian Archive, Library and Museum Authority.

CONFLICT OF INTEREST

No conflict of interest was declared.

ORCID

Terje Grøntoft https://orcid.org/0000-0002-6200-9460

ENDNOTE

[1] At the time of the regression analysis (2006) called «Statistical package for the Social Sciences". Acquired by IBM in 2009 and now called "Statistical Product and Service Solutions".

REFERENCES

1. Nazaroff WW, Weschler CJ. Indoor acids and bases. *Indoor Air*. 2021;30:559-644. doi:10.1111/ina.12670
2. Camuffo D, Brimblecombe P, Van Grieken R, et al. Indoor air quality at the Correr Museum, Venice, Italy. *Sci Total Environ*. 1999;236:135-152. doi:10.1016/s0048-9697(99)00262-4
3. Brimblecombe P, Blades ND, Camuffo D, et al. The indoor environment of a modern Museum building, The Sainsbury Centre for Visual Arts, Norwich, UK. *Indoor Air*. 1999;9:146-164.
4. Weschler SJ, Shields HC, Naik DV. Indoor chemistry involving O_3, NO and NO_2 as evidenced by 14 months of measurements at a site in Southern California. *Environ Sci Technol*. 1994;194(23):2120-2132. doi:10.1021/es00061a021
5. Carslaw N. A new detailed chemical model for indoor air pollution. *Atmos Environ*. 2007;41:1164-1179. doi:10.1016/j.atmosenv.2006.09.038
6. Nazaroff WW, Cass GR. Mathematical modelling of chemically reactive pollutants in indoor air. *Environ Sci Technol*. 1986;20:924-934. doi:10.1021/es00151a012
7. Cheung JL, Li YQ, Boniface J, et al. Heterogeneous interactions of NO_2 with aqueous surfaces. *J Phys Chem A*. 2000;104:2655-2662. doi:10.1021/jp992929f
8. Finlayson-Pitts BJ, Wingen LM, Sumner AL, Syomin D, Ramazan KA. The heterogeneous hydrolysis of NO_2 in laboratory systems and in outdoor and indoor atmospheres: an integrated mechanism. *Phys Chem Phys*. 2003;5(2):223-242. doi:10.1039/B208564J
9. Spicer CW, Buxton BE, Holdren MW, et al. *Variability and Source Attribution of Hazardous Urban Air Pollutants*. Battelle; 1993.
10. Weschler SJ, Shields HC. Potential reactions among indoor pollutants. *Atmos Environ*. 1997;31(21):3487-3495. doi:10.1016/S1352-2310(97)00219-7
11. Weschler SJ, Brauer M, Koutrakis P. Indoor ozone and nitrogen dioxide: a potential pathway to the generation of nitrate radicals, dinitrogen pentaoxide, and nitric acid indoors. *Environ Sci Technol*. 1992;26(1):179-184. doi:10.1021/es00025a022
12. Druzik JR, Adams MS, Tiller C, Cass GR. The measurement and model predictions of indoor ozone concentrations in museums. *Atmos Environ*. 1990;24:1813-1823. doi:10.1016/0960-1686(90)90513-M
13. Guo Z. Development of a Windows based indoor air quality simulation software package. *Environ Model Softw*. 2000;15:4003-4010.
14. Sheir FH, Heitner KL. Theoretical model for relating indoor pollutant concentrations to those outside. *Environ Sci Technol*. 1973;8(5):444-451.
15. Cass GR, Nazaroff WW. Mathematical modelling of chemically reactive pollutants in indoor air. *Environ Sci Technol*. 1986;20(9):924-934. doi:10.1021/es00151a012
16. Drakou G, Zerefos G, Ziomas I, Voyatzaki M. Measurements and numerical simulations of indoor O_3 and NOx in two different cases. *Atmos Environ*. 1998;32(4):595-610.
17. Wang ZX. A modelling study of the impact of photolysis on indoor air quality. Department of Environment and Geography. UK: University of York; 2021.
18. Wang ZX, Kowal SF, Carslaw N, Kahan TF. Photolysis-driven indoor air chemistry following cleaning of hospital wards. *Indoor Air*. 2020;30:1241-1255.
19. Weschler SJ. Ozone in indoor environments: concentration and chemistry. *Indoor Air*. 2000;10:269-288. doi:10.1034/j.1600-0668.2000.010004269.x
20. Weschler SJ, Shields HC, Naik DV. Indoor ozon exposures. *J Air Pollut Control Assoc*. 1989;39:1562-1568. doi:10.1080/08940630.1989.10466650
21. Zhou S, Young CJ, VandenBoer TC, Kowal SF, Kahan TF. Time resolved measurements of nitric oxide, nitrogen dioxide, and nitrous acid in an occupied New York home. *Environ Sci Technol*. 2018;52:8355-8364. doi:10.1021/acs.est.8b01792
22. Røyset R. Comparison of passive and active sampling methods for the determination of nitrogen dioxide in urban air. *Fresenius J Anal Chem*. 1997;360:69-73. doi:10.1007/S002160050644
23. Dahlin E, Grøntoft T, Rentmeister S, et al. Development of an early warning sensor for assessing deterioration of organic materials indoor in museums, historic buildings, and archives. In: 14th triennial meeting, The Hague, 12–16 September 2005, preprints volume II, ICOM Committee for Conservation, James & James/Earthscan, London, pp. 617–624; 2005. Accessed February 07, 2022. https://www.nilu.no/apub/8404/
24. European Environmental Agency (EEA). Air quality statistics - expert viewer; 2021. Accessed August 2, 2021. https://www.europa.eu/data-and-maps/dashboards/air-quality-statistics-expert-viewer
25. European Environment Agency (EEA). Premature deaths attributable to air pollution; 2020. Accessed February 07, 2022. https://www.eea.europa.eu/media/newsreleases/many-europeans-still-exposed-to-air-pollution-2015/premature-deaths-attributable-to-air-pollution
26. Gardiner B. Air pollution kills millions every year, like a 'pandemic in slow motion. April 2021 issue of National Geographic magazine; 2021. Accessed February 07, 2022. https://www.nationalgeographic.com/magazine/article/air-pollution-kills-millions-every-year-like-a-pandemic-in-slow-motion-feature
27. Meng X, Liu C, Chen R, et al. Short term associations of ambient nitrogen dioxide with daily total, cardiovascular, and respiratory mortality: multilocation analysis in 398 cities. *BMJ*. 2021;372:n534. doi:10.1136/bmj.n534
28. World Health Organization. Air pollution. 2022. Accessed February 07, 2022. https://www.int/health-topics/air-pollution#tab=tab_1
29. Grosjean D, Whitmore PM, De Moor CP, Cass GR, Druzik JR. Fading of alizarin and related artists' pigments by atmospheric ozone. *Environ Sci Technol*. 1987;21(7):635-643. doi:10.1021/es00161a003
30. Lynn Y, Salmon G, Cass G. The ozone fading of traditional Chinese plant dyes. *J AIC*. 2000;39:245-257. doi:10.1179/019713600806082685
31. Saito M, Goto S, Kashiwagi M. Effect of the concentration of NO_2 gas to the fading of plant dyes. *Sci Papers Jpn Antiques Art Crafts*. 1993;38:1-9.

32. Saito M, Goto S, Kashiwagi M. Effect of the concentration on NO_2 gas to the fading of fabrics dyed with natural dyes. *Sci Papers Jpn Antiques Art Crafts*. 1994;39:67-74.
33. Whitmore PM, Cass GR. The fading of artists' colorants by exposure to atmospheric nitrogen dioxide. *Stud Conserv*. 1989;34(2):85-97. doi:10.2307/1506270
34. Whitmore P, Cass GR, Druzik JR. The ozone fading of traditional natural organic colorants on paper. *J Am Inst Conserv*. 1987;26:45-58. doi:10.1179/019713687806027906
35. Drisko K, Cass GR, Whitmore PM, Druzik JR. Fading of artists' pigments due to atmospheric ozone. In: Vendl A, Pichler B, Weber J, Banik G, eds. *Wiener Berichte über Naturwissenschaft in der Kunst 2–3* ACS(American Chemical Society) Publications. 1985: 6–89. Accessed May 26, 2021. https://core.ac.uk/download/pdf/33113605.pdf
36. Shaver CL, Cass GR, Druzik JR. Ozone and the deterioration of works of art. *Environ Sci Technol*. 1983;17:748-752. doi:10.1021/es00118a011
37. Druzik J. Ozone: the intractable problem. *WAAC Newsletter*. 1985;7:3-9. Accessed May 26, 2021. https://cool.culturalheritage.org/waac/wn/wn07/wn07-3/wn07-302.html
38. Adelstein PZ, Zinn ED, Reilly JM. Effect of atmospheric pollution on paper stability. *J Pulp Pap Sci*. 2003;29:1.
39. Menart E, de Bruin G, Strlič M. Effects of NO_2 and acetic acid on the stability of historic paper. *Cellulose*. 2014;21:3701-3713. doi:10.1007/s10570-014-0374-4
40. Reilly J, Zinn E, Adelstein P. *Atmospheric pollutant aging test method development. Final report to American society for testing materials*. Image permanence institute at Rochester Institute of Technology; 2001:52-97.
41. Bonaduce I, Odlyha M, Di Girolamo F, Lopez-Aparicio S, Grontoft T, Colombini P. The role of organic and inorganic indoor pollutants in museum environments in the degradation of dammar varnish. *Analyst*. 2013;138:487-500. doi:10.1039/c2an36259g
42. Arroyave C, Morcillo M. The effect of nitrogen oxides in atmospheric corrosion of metals. *Corros Sci*. 1995;37(2):293-305. doi:10.1016/0010-938X(94)00136-T
43. Chen Z, Liang D, Ma G, Frankel GS, Allen HC, Kelly RG. Influence of UV irradiation and ozone on atmospheric corrosion of bare silver. *Corros Eng Sci Technol*. 2010;45:169-180. doi:10.1179/147842209X12579401586681
44. Kucera V, Tidblad J, Kreislova K, et al. UN/ECE ICP Materials dose-response functions for the multi-pollutant situation. *Water Air Soil Pollution*. 2007;7:249-258. doi:10.1007/s11267-006-9080-z
45. Tétreault J. *Airborne Pollutants in Museums, Galleries, and Archives: Risk Assessment, Control Strategies, and Preservation Management*. Canadian Conservation Institute; 2003.
46. Blades N, Oreszczyn T, Bordass B, Cassar M. *Guidelines on pollution control in museum buildings*; 2000. Published by the Museums Association and distributed with MUSEUM PRACTICE, 15, Nov. London.
47. Hatchfield PB. *Pollutants in the Museum Environment*. Archetype Publications Ltd; 2002.
48. Baij L, Chassouant L, Hermans JJ, Keune K, Iedemaa PD. The concentration and origins of carboxylic acid groups in oil paint. *RSC Adv*. 2019;9:35559. doi:10.1039/c9ra06776k
49. Colombini MP, Modugno F, Fuoco R, Tognazzi A. A GC-MS study on the deterioration of lipidic paint binders. *Microchem J*. 2002;73:175-185. doi:10.1016/S0026-265X(02)00062-0
50. Schaich KM. Lipid oxidation: new perspectives on an old reaction. In: *Edible oil and fat products: Chemistry, properties, and safety aspects*. Wiley Online LIbrary; 2020.
51. Modugno F, Di Gianvincenzo F, Degano I, van der Werf ID, Bonaduce I, van den Berg KJ. On the influence of relative humidity on the oxidation and hydrolysis of fresh and aged oil paints. *Sci Rep*. 2019;2019(9):5533. doi:10.1038/s41598-019-41893-9
52. Ferm M & Bloom E Use of diffusive sampling in museums and archives; Accessed May 28, 2021. Swedish Environmental Research Institute; 2010. http://iaq.dk/iap/iaq2010/iaq2010_ferm_poster.pdf
53. Grøntoft T, Henriksen JF, Hansen JE, et al. MASTER (EVK4-CT-2002-00093) Preventive Conservation Strategies for Protection of Organic Objects in museums Historic Buildings and Archives. Project Deliverable no D.3.1, WP 3. Sensor and Environmental Data from the Field Test Programme. Unpublished. NILU OR, 45/2009; 2009. Can be obtained on contacting NILU-Norwegian Institute for Air Research. Accessed February 07, 2022. https://www.nilu.no/apub/24477/
54. Elsec. *765 Environmental Monitor. User Manual*. Littlemore Scientific Engineering, Dorset, UK: Elsec; 2011. Accessed February 07, 2022. https://www.talasonline.com/images/PDF/Manuals/765Manual.pdf
55. Brimblecombe P. The composition of museum atmospheres. *Atmos Environ*. 1988;24(1):1-8. doi:10.1016/0957-1272(90)90003-D
56. Cano-Ruiz JA, Kong D, Balas RB, Nazaroff WW. Removal of reactive gases at indoor surfaces. Combining mass transport and surface kinetics. *Atmos Environ*. 1993;27:2039-2050. https://www.academia.edu/5462874/Removal_of_reactive_gases_at_indoor_surfaces_Combining_mass_transport_and_surface_kinetics
57. Grøntoft T, Raychaudhuri MR. Compilation of tables of surface deposition velocities for O_3, NO_2 and SO_2 to a range of indoor surfaces. *Atmos Environ*. 2004;38(4):533-544.
58. Liu D-L, Nazaroff WW. Modeling pollutant penetration across building envelopes. *Atmos Environ*. 2001;35:4451-4462. doi:10.1016/S1352-2310(01)00218-7
59. Atkinson R. Evaluated kinetic and photochemical data for atmospheric chemistry supplement IV. IUPAC Subcommittee on Gas Kinetic Data Evaluation for Atmospheric Chemistry. *J Phys Chem Ref Data*. 1992;21(6):1125-1568: doi:10.1063/1.555918
60. Seinfeld JH, Pandis SP. *Atmospheric Chemistry and Physics. From Air Pollution to Climate Change*. John Wiley & Sons, Inc.; 2016.
61. London Air. Imperial College London, 2021. Accessed February 07, 2022. https://www.londonair.org.uk/london/asp/AnnualMaps.asp?Species=O3
62. Hales CH, Rollinson AM, Shair FH. Experimental verification of linear combination model for relating indoor-outdoor pollutant concentrations. *Environ Sci Technol*. 1974;8:452-453. doi:10.1021/es60090a007
63. Salmon LG, Cass GR, Bruckman K, Haber J. Ozone exposure inside museums in the historic central district of Krakow, Poland. *Atmos Environ*. 2000;34:3823-3832. doi:10.1016/S1352-2310(00)00107-2
64. Fiadzomor P. Industrial placement report, Gas standards for indoor and in-car air, VAM 1.8 project, DTI ITT Number GBBK/C/14/26; 2002.
65. Garnham C. An investigation into light intensity in the UK. *Brit Cact Succ J*. 1999;17(3):154-156. http://www.jstor.org/stable/42794701
66. Global Solar Atlas. Global Photovoltaic Power Potential by Country; 2022. https://globalsolaratlas.info/global-pv-potential-study
67. Spławińska M. Factors determining seasonal variations in traffic volumes. *Arch Civil Eng*. 2017;63(4):35-50. doi:10.1515/ace-2017-0039
68. Stathopoulos A, Karlaftis M. Temporal and spatial variations of real-time traffic data in urban areas. *Transp Res Rec J Transp Res Board*. 2001;1768(1):135-140. doi:10.3141/1768-16
69. Simpson D, Fagerli H, Jonson JE, Tsyro S, Wind P. Transboundary Acidification, Eutrophication and Ground Level Ozone in Europe PART I. Unified EMEP Model Description. EMEP Status Report 1/2003. Norwegian Meteorological Institute; 2003. Accessed May 26, 2021. http://www.emep.int/publ/reports/2003/emep_report_1_part1_2003.pdf
70. Walker S-E, Solberg S, Denby B. Development and implementation of a simplified EMEP photochemistry scheme for urban areas in

EPISODE. NILU (Norwegian Institute for Air Research) report. TR 13/2003. 2003. Accessed May 26, 2021. https://www.nilu.no/wp-content/uploads/dnn/13-2003-sew-sso-bde.pdf
71. Eclipsofile Global cloud cover. 2022. Accessed 07 February 2022. https://eclipsophile.com/global-cloud-cover/
72. Leemans R, Cramer W. The IIASA database for mean monthly values of temperature, precipitation and cloudiness on a global terrestrial grid. Research Report RR-91–18. November. International Institute of Applied Systems Analysis, Laxenburg, pp. 61. Accessed May 26, 2021. http://pure.iiasa.ac.at/id/eprint/3482/
73. Meerkötter R, König C, Bissolli P, Gesell G, Mannstein H. A 14-year European Cloud Climatology from NOAA/AVHRR data in comparison to surface observations. *Geophys Res Lett*. 2004;31:L15103. doi:10.1029/2004GL020098
74. Bikundia DS, Pancholi P, Kumar A, Chourasiya S. An observation of seasonal and diurnal behavior of O_3-NO_x relationships and local/regional oxidant ($OX = O_3 + NO_2$) levels at a semi-arid urban site of western India. *Sustain Environ Res*. 2018;28:79-89. doi:10.1016/j.serj.2017.11.001
75. IMPACT. Online tools for preventive conservation. UCL Institute for Sustainable Heritage; 2021. Accessed November 3, 2021 (in the process of being reprogrammed). https://www.ucl.ac.uk/bartlett/heritage/online-tools-preventive-conservation
76. Kruppa D, Blades N, Cassar M. A web-based software tool for predicting the levels of air pollutants inside museum buildings developed by the EC impact project. Presented at: Cultural Heritage Research: a Pan-European Challenge, 5th EC Conference, Cracow, Poland; 2002. Accessed November 3, 2021. https://discovery.ucl.ac.uk/id/eprint/4604/

SUPPORTING INFORMATION

Additional supporting information may be found in the online version of the article at the publisher's website.

How to cite this article: Grøntoft T. The influence of photochemistry on outdoor to indoor NO_2 in some European museums. *Indoor Air*. 2022;32:e12999. doi:10.1111/ina.12999